Advanced Review

Tambora 1815 as a test case for high impact volcanic eruptions: Earth system effects

Christoph C. Raible,[1,2†] Stefan Brönnimann,[1,3†*] Renate Auchmann,[1,3] Philip Brohan,[4] Thomas L. Frölicher,[5] Hans-F. Graf,[6] Phil Jones,[7,8] Jürg Luterbacher,[9,14] Stefan Muthers,[1,2] Raphael Neukom,[1,3] Alan Robock,[10] Stephen Self,[11] Adjat Sudrajat,[12] Claudia Timmreck[13] and Martin Wegmann[1,3]

Edited by Matilde Rusticucci, Domain Editor, and Mike Hulme, Editor-in-Chief.

The eruption of Tambora (Indonesia) in April 1815 had substantial effects on global climate and led to the 'Year Without a Summer' of 1816 in Europe and North America. Although a tragic event—tens of thousands of people lost their lives—the eruption also was an 'experiment of nature' from which science has learned until today. The aim of this study is to summarize our current understanding of the Tambora eruption and its effects on climate as expressed in early instrumental observations, climate proxies and geological evidence, climate reconstructions, and model simulations. Progress has been made with respect to our understanding of the eruption process and estimated amount of SO_2 injected into the atmosphere, although large uncertainties still exist with respect to altitude and hemispheric distribution of Tambora aerosols. With respect to climate effects, the global and Northern Hemispheric cooling are well constrained by proxies whereas there is no strong signal in Southern Hemisphere proxies. Newly recovered early instrumental information for Western Europe and parts of North America, regions with particularly strong climate effects, allow Tambora's effect on the weather systems to be addressed. Climate models respond to prescribed Tambora-like forcing with a strengthening of the wintertime stratospheric polar vortex, global cooling and a slowdown of the

[†]These authors contributed equally.

*Correspondence to: stefan.broennimann@giub.unibe.ch

[1]Oeschger Centre for Climate Change Research, University of Bern, Bern, Switzerland

[2]Climate and Environmental Physics, University of Bern, Bern, Switzerland

[3]Institute of Geography, University of Bern, Bern, Switzerland

[4]Met Office Hadley Centre, Exeter, UK

[5]Environmental Physics, Institute of Biogeochemistry and Pollutant Dynamics, ETH Zürich, Zürich, Switzerland

[6]Geography Department, Centre for Atmospheric Science, University of Cambridge, Cambridge, UK

[7]Climatic Research Unit, University of East Anglia, Norwich, UK

[8]Department of Meteorology, Center of Excellence for Climate Change Research, King Abdulaziz University, Jeddah, Saudi Arabia

[9]Department of Geography, Climatology Climate Dynamics and Climate Change, Justus Liebig University of Giessen, Giessen, Germany

[10]Department of Environmental Sciences, Rutgers University, New Brunswick, NJ, USA

[11]Department of Earth and Planetary Science, University of California, Berkeley, CA, USA

[12]Department of Geology, Padjadjaran University, Bandung, Indonesia

[13]Max Planck-Institute for Meteorology, Hamburg, Germany

[14]Centre for International Development and Environmental Research, Justus Liebig University Giessen, Giessen, Germany

Conflict of interest: The authors have declared no conflicts of interest for this article.

water cycle, weakening of the summer monsoon circulations, a strengthening of the Atlantic Meridional Overturning Circulation, and a decrease of atmospheric CO_2. Combining observations, climate proxies, and model simulations for the case of Tambora, a better understanding of climate processes has emerged.

How to cite this article:
WIREs Clim Change 2016. doi: 10.1002/wcc.407

INTRODUCTION

In April 1815, the dormant volcano Tambora on the Indonesian island of Sumbawa (8.25°S, 118.00°E; Figure 1) erupted violently. The eruption immediately killed thousands of people on Sumbawa. During the following months, tens of thousands died of starvation and disease on Sumbawa and neighboring islands. The gas plume of this enormous eruption, the largest since the 1257 Samalas eruption (shown as Rinjani in Figure 1), produced stratospheric sulfate aerosols that shielded incoming solar radiation over the following 3 years.[1] The aerosols led to a substantial annual cooling of the Tropics and the extratropical Northern Hemisphere by approximately 0.4–0.8°C relative to the preceding 30 years.[2–4] The following year, 1816, went down in history as a 'Year without a Summer,[5–7] resulting in large socioeconomic impacts such as crop failures and associated famines, across the Northern Hemisphere, including China, North America, and Europe.[8–11] Given these worldwide impacts, the Tambora eruption must be considered to have had one of the greatest death tolls attributed to a volcanic eruption.

The Tambora eruption and its climatic consequences were studied repeatedly over the past century with respect to diverse research questions ranging from ice age theory,[12] asteroid impacts, nuclear winter, and others.[13] A first comprehensive overview of the Tambora effects was published in 1992. The book by Harington[7] compiled the findings with respect to imprints in proxies, climate data, and societal impacts across various disciplines, constituting an authoritative reference on Tambora impacts. However, much has been learned since the publication of Harington (1992) using new palaeoclimatological evidence from different archives, newly digitized instrumental data and documentary evidence, and particularly using coupled climate models. The bicentenary of the Tambora eruption provides an opportunity to revisit the event and revisit our understanding of its effects on climate.

As an 'experiment of nature,[14] the Tambora eruption allows current scientists to test hypotheses on the interaction between the solid Earth and the atmosphere, atmospheric chemistry and physics, dynamics and radiation, stratosphere and troposphere, atmosphere and oceans, climate and biosphere, climate and society, and many others. Because of its magnitude and its severe impacts, Tambora may provide additional insights to those obtained from studying more recent, better observed eruptions. These new insights contribute to better process understanding, help to project the possible consequences of future eruptions, and may be

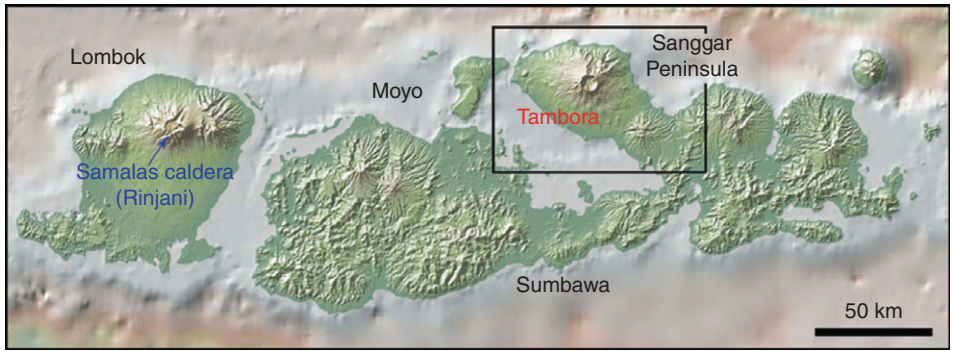

FIGURE 1 | Map of the Lombok–Sumbawa sector of the Sunda arc, Indonesia, showing the location of Tambora and Rinjani, the sites of the probably two largest eruptions of the last millennium. The map was generated using GeoMapApp©. (Reprinted with permission from Ref 145. Copyright 2015 John Wiley and Sons)

relevant for assessing geoengineering options. In particular, Tambora is a good test case for studying historical climate-society interactions. Tambora erupted at the beginning of the early instrumental period so that making best use of observations, proxy information, reconstructions, model simulations, and historical evidence is essential and thus calls for a multidisciplinary approach. This paper focuses on the physical processes.

The paper first provides an overview of the eruption, stratospheric aerosols, and radiative forcing (second section). This section is based on volcanological evidence on the eruption and eyewitness accounts, but also evidence from environmental archives such as sulfate from polar ice cores. The analysis includes comparisons with well-observed eruptions including Pinatubo (1991), as well as computer model results. The third section focuses on early instrumental data and derived summer temperature, precipitation, and sea-level pressure reconstructions for the North Atlantic and Europe for which the most abundant information is available. The Following section then analyzes the climatic imprint of the Tambora eruption in various natural archives such as tree rings, ice cores, or sediments. The fifth section summarizes climate model studies of the Tambora eruption and large volcanic eruptions in general, as models are an important tool to address the underlying mechanisms. Finally, we present conclusions and summarize from a present day perspective what we can learn from the Tambora event.

THE TAMBORA ERUPTION, AEROSOLS, AND RADIATIVE FORCING

Tambora is a massive, shield-like volcano that occupies much of the Sanggar Peninsula in northern Sumbawa, part of the Lesser Sunda Islands in Indonesia (Figure 1). The volcano reaches a height of 2850 m, but before 1815, it may have been one of Indonesia's highest mountains, more than 4000 m in elevation.[15]

The climactic phase of the eruption on April 10–11, 1815,[1,16] which followed almost a week of minor and intermittent explosions, caused the summit to collapse, forming a caldera 6×7 km wide and more than 1 km deep (Figure 2).

The 1815 Tambora eruption is probably the largest caldera-forming eruption of the last few centuries. Recent estimates suggest an erupted magma (dense rock equivalent; DRE) volume of ~30–50 km^3.[1,17] It is thought that this magma was a relatively homogeneous trachyandesite that was stored in a shallow crustal reservoir before the eruption. During the eruption, pyroclastic flows swept down all flanks of the volcano and into the sea extending the coastline of the Sanggar Peninsula. The pyroclastic flows and related phenomena were mainly responsible for the casualties on Sumbawa Island. Pumice and coarse ash fell close to the volcano on the Sanggar Peninsula, but according to eyewitness accounts the finest volcanic ash fell as far as western Java, at least 1300 km from the source, and much was deposited into the sea. Remobilization of the volcanic deposits on land, and the fact that a significant portion of the 1815 ejecta flowed or fell into the sea, make an accurate determination of the eruption volume difficult. For some, if not most of the older large Holocene eruptions, some of which were likely to be significantly larger than Tambora, the erupted volumes reported may be even less accurate.

On the basis of the above uncertainties, the measured sulfur content of both the pre-eruption volatile content (from measurements on inclusions in crystals in the 1815 tephra deposit) and degassed magma (from measurements on volcanic glass in the deposit) gives an emitted SO_2 mass of about 60 Mt (Tg) at the low end of the range of volumes,[18] or larger if the true volume is shown to be bigger.

The stratigraphy of tephra deposits explored about 25 km from the Tambora summit sheds some

FIGURE 2 | The 7 × 6 km wide and more than 1-km deep summit caldera of Tambora created by the 1815 eruption. The 1815 eruptive products form the top of the caldera wall, as seen in the foreground. On the floor of the caldera lie an ephemeral lake and a small cone from a post-1815 eruption. Photo by Katie Preece. (Reprinted with permission from Ref 145. Copyright 2015 John Wiley and Sons)

light on the sequence of eruption phases.[16] Prior to the cataclysmic eruption on April 10, 1815, a series of less intense phreatomagmatic and Plinian eruptions took place with maximum intensity of the eruption exceeding 10^8 kg s^{-1}, leading to maximum plume heights of more than 30 km. The eruption culminated in the climactic eruption of April 10–11 with an intensity of probably 3×10^8 kg s^{-1} and a maximum plume height of more than 40 km.[16] However, this arguably reflects overshoot heights rather than the altitude at which the bulk of the gases was injected.[19] The huge Plinian eruption column collapsed and formed giant pyroclastic flows from which the main co-ignimbrite or Phoenix plume arose. This sequence of events is essential for the atmospheric injection height of SO_2 and fine ash. Observations after more recent big eruptions and model simulations[20] show that the vertical profiles of SO_2 and fine ash injection have maxima near the neutral buoyancy height (NBH), which is significantly lower than the maximum plume height. During Plinian phases, when the convection of the plume is well organized, initial momentum and heat propel fine ash and gases to heights above the NBH, but most of the material will fall back to the NBH, forcing a spread of the plumed umbrella that can exceed 100 m s^{-1}, leading to very fast horizontal transport of ash at NBH and distant ash fall afterwards. If the mass load within the plume becomes too high, the plume starts collapsing and feeds pyroclastic flows rapidly surging down the flanks of the volcano for tens of kilometers and filling the near-surface atmosphere with a mixture of hot gases and ash.

From this 'hot pillow,' very fine ash particles and gases will be elutriated and form another, secondary eruption column, the Phoenix or co-ignimbrite cloud. Owing to the spatial extent of this Phoenix cloud, convection is less organized and the NBH is lower than for the original Plinian plume. Merger of both will lead to hybrid plumes. The plume dynamics depend on a wide range of in-plume processes such as condensation and freezing of water with formation of hydrometeors and latent heat release, aggregation of ash particles, rainout, washout and freeze-out of gases and particles, electric charging, of which, for historic eruptions, we are mostly lacking observed information. Such events were simulated for eruptions close to the Tambora eruption rates.[21] For mass eruption rates of 1.3×10^8 kg s^{-1} van Eaton et al.[21] found NBH based on maximum ash concentration of about 13 km for dry co-ignimbrite plumes and around 22 km for Plinian columns with initial water content of 10%. For mass eruption rates of 1.1×10^9 kg s^{-1}, they found NBH based on maximum ash concentration of about 18 km for dry co-ignimbrite plumes and around 23 km for Plinian columns. Maximum eruption heights for these cases were simulated to about 32–42 km, that is, much higher than the NBH. Gas injection heights are generally slightly higher than ash injection heights. For the Tambora mass eruption rates, we can therefore assume a vertical profile with a maximum injection of SO_2 between 20 and 25 km. This corresponds well with observed injection height profiles after the smaller 1991 Pinatubo eruption.

The sulfate aerosol cloud that developed from the injected SO_2 was spread globally by the stratospheric winds. The stratospheric meridional circulation transported the aerosols poleward. Ultimately, the sulfate reached the troposphere, where it was quickly washed out. Today, Tambora's sulfate signal is still preserved in polar ice cores. In fact, estimates of sulfate mass fluxes from bipolar ice cores provide the basis for reconstructing stratospheric sulfur amounts and of radiative forcing. However, this requires an assumption on the efficiencies of stratospheric transport in each hemisphere. While Gao et al.[22] found an approximately equal distribution of sulfate deposition in Antarctic and Greenland ice cores, Sigl et al.[23] suggested considerably higher sulfate fluxes in Antarctica as compared to Greenland. This appears inconsistent with the fact that climate effects were arguably much stronger in the Northern Hemisphere than the Southern Hemisphere (*Proxies and Proxy-Based Reconstructions* section). In a two-dimensional aerosol model study using a sulfate injection rate determined from ice cores, Arfeuille et al.[19] found a strongly asymmetric distribution of hemispheric aerosol loading after the Tambora eruption. Owing to the timing of the Tambora eruption, at the start of the Southern Hemisphere winter season, they found that the majority of the aerosol load was transported southward, albeit stratospheric circulation in 1815 is of course unknown and was prescribed in the model based on more recent data. The hemispheric partitioning of aerosols thus remains an open question. Greenland and Antarctic deposition efficiencies (the ratio of sulfate flux to each ice sheet to the maximum hemispheric stratospheric sulfate aerosol burden) vary as a function of the magnitude and season of stratospheric sulfur injection.[24]

Based on ice core-based estimates, the Tambora SO_2 injection was about 3.5 times larger than the 1991 Pinatubo eruption, but the resulting radiative forcing was only about two times higher, assuming that the larger SO_2 injection produced larger aerosol particles, with resulting smaller lifetimes and less

impact on radiation per unit mass.[19,25] The peak net radiative forcing from Tambora was about −5 W m^{-2} (defined as global downward short-wave radiative forcing at the tropopause[25] or global top-of-atmosphere downward net radiation anomalies[26,27]). The climate response to this thick aerosol cloud is discussed in the following sections.

CLIMATE RESPONSE IN OBSERVATIONS

Widespread meteorological observations across much of Western and Central Europe began in the 1780s.[28] Longer series have been developed at the monthly timescale for a number of locations extending back to the 17th century.[29–32] More recent work has seen this development extended to the daily timescale[33–37] ranging from Iberia in the west to European Russia in the east. By the 18th century, efforts to develop distinct meteorological networks had emerged due to the urgings and coordination of the *Royal Society in England* (by the Society's Secretary James Jurin), from the medical fraternity in France (by the *Societe Royale de Medecine* 1776–1789), in Bavaria (by the *Bavarian Academy of Science* 1781–1789, in the *Bayerische Ephemeriden*) and across Europe (under the *Societas Meteorologica Palatina in Mannheim*, 1781–1792), even enabling weather maps to be drawn for this decade.[38] The Mannheim Ephemerides, reporting subdaily meteorological observations from a network of up to 50 stations, ended in 1792 due to the Napoleonic Wars, and the availability of material for the 1800s and 1810s is somewhat less extensive than the two earlier decades and since the 1820s. Briffa and Jones[39] presented temperature anomaly maps for the four seasons during 1816 and for the 1810s (1810–1819) with respect to 1951–1970 for temperature and 1921–1960 for precipitation. These were based on 46 temperature and 29 precipitation series. The precipitation series were restricted to Poland westwards, but temperature data were available at Archangel, Vilnius, St Petersburg, Kiev and Kazan east of Poland. In Figure 3, we update these results using more recently produced series from Europe and extend the independently reconstructed sea-level pressure, temperature, and precipitation maps[32,40] to encompass more areas of the North-Atlantic-European region than available in 1992.

Atmospheric circulation in the summer of 1816 was characterized by a weak Azores high and a strong Icelandic low (Figure 3, top). Sea-level pressure reconstructions based on land station pressure series and information from ship log books from the eastern North Atlantic[40] reveal below normal pressure over the North Atlantic European region (30°W–40°E and 30°–70°N) connected with more frequent low-

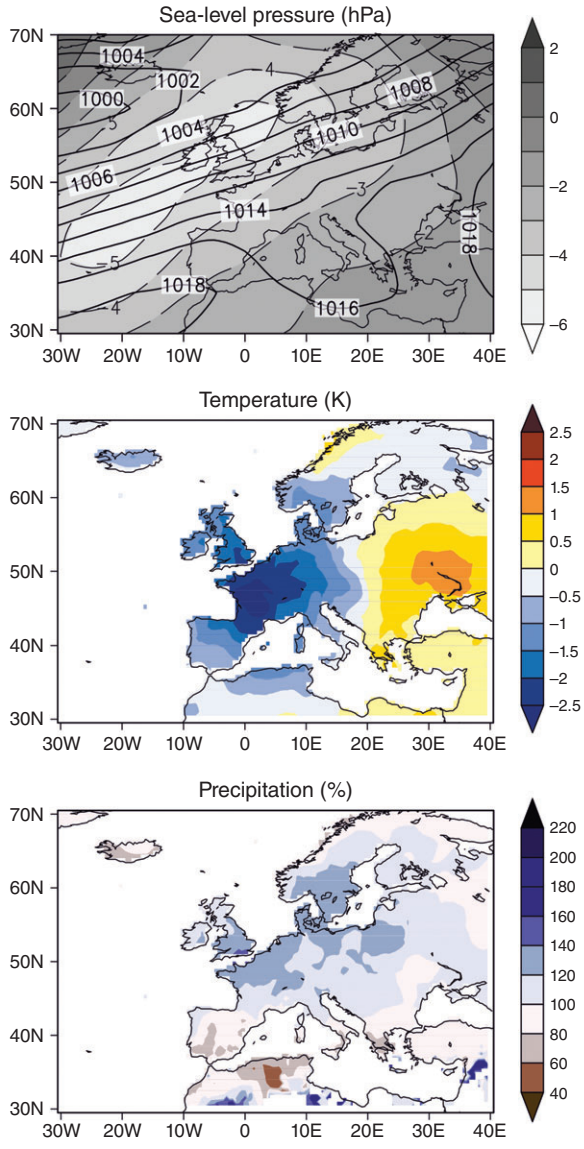

FIGURE 3 | (Top): Sea-level pressure (contour lines, in hPa) and anomalies (stippled lines; in hPa) for summer (June-August) 1816 statistically reconstructed using station pressure series in combination with ship log book information from the northeastern North Atlantic (data from Küttel et al.[40]). (Middle): temperature anomalies (in °C) for summer 1816 statistically reconstructed using station temperature series only (data from Casty et al.[32]). (Bottom): precipitation (in % of the 1961–1990 average) for summer 1816 statistically reconstructed using station precipitation series only (data from Casty et al.[32]). Temperature and precipitation reconstructions in the outer margins of Europe and the Mediterranean are less certain due to the lack of meteorological station information for those areas. All anomalies are with respect to 1961–1990.

pressure systems and generally a stronger westerly and northwesterly air flow toward Europe.

For temperature (Figure 3, middle), the most anomalous cold summer temperatures were centered on Switzerland and eastern France. The summer of 1816 was one of the coldest summers measured over much of Western Europe from Central Scandinavia to the Mediterranean. Further east the few series in Russia and the Ukraine indicate a milder summer in 1816. This might be due to more southerly atmospheric flow from Northern Africa through Turkey to western Russia (Figure 3, top). Anomalous low pressure over large parts of the North Atlantic and Europe (Figure 3, top) was connected with excessive rainfall across most of Western Europe, north of the Mediterranean. Particularly in southeast England and northeastern France (Figure 3, bottom), this summer was most anomalously wet. European instrumental averages indicate that the 1810s were the coldest decade since comparable records began in the 1780s. Most years within the 1810s would be classed as cold (relative to 1961–1990), but 2 years, 1814 and 1816 stand out as being exceptionally cold. Part of this was probably due to the unknown eruption in 1808/1809[41] that is clearly evident in ice core series.[23]

The year without a summer of 1816 has also been extensively studied in these single site records (see papers in Harington[7]). More recent work has used series where the subdaily data have now been digitized.[42,43] The analysis of twice-daily data from Geneva,[42] which is located in the region with the largest negative temperature anomaly in 1816 in Europe (see Pfister,[44] Trigo et al.,[45] and Figure 3), shows that the afternoon temperature anomalies (compared to the contemporary reference period 1799–1821, without the volcanically perturbed years 1809–1811 and 1815–1817) were more strongly affected than the morning temperatures. The entire distribution of temperature anomalies was shifted by −3.8°C compared to the reference period. For the sunrise temperature, a smaller shift (-1.8°C) was found, with a distinct narrowing of the distribution. Extremely low sunrise temperatures were as rare in 1816 as in the reference period, but warmer than average sunrise temperatures were missing.[42] Both the larger change in afternoon temperatures and the change in the distribution can be explained by an increase in cloud cover, which is well documented and can in turn be related to a significant change in weather types. For Geneva, a tripling of 'low pressure' situations and an absence of 'high pressure' situations was observed as illustrated by the pressure reconstruction in Figure 3. Precipitation in Geneva in summer 1816 increased by 80% but with no change in the intensity distribution, that is, the frequency of precipitation days increased.[42] Analysis of this single site suggests that the summer 1816 was characterized by extreme climate (weather types statistics) and not extreme weather (the tails of the distributions were not much affected). Subdaily pressure data from around 50 sites in Europe and North America show an increased synoptic activity (measured by a 2–6 days bandpass filter and expressed relative to a present day climatology) in a band stretching from western France to Austria. This suggests increased storminess due to frequent passages of storms, consistent with the space-time pattern of precipitation.[43] These anomalies in weather patterns found in the observations are qualitatively consistent with model studies (see Section MODELING THE CLIMATE EFFECT OF THE TAMBORA ERUPTION), although presumably a large fraction of unforced variability contributed.

Other long daily series across Europe have also been analyzed. The most well-known temperature series is the Central England Temperature (CET) series, which extends back on a monthly timescale to 1659 and to 1772 at the daily timescale.[46] Focusing just on the JJA summer, 1816 stands out as the coldest summer of the 1810s and in the long CET series as the third coldest summer since 1659 (colder summers were measured in 1725 and 1695). Figure 4 shows the daily temperatures during 1816 compared to those in the most recent complete year (2014) which was the warmest year in the CET series. For 1816 only a few days were above the 1961–90 period, with only 1 week in the spring and summer (in late April) being above. 2014, in contrast, experienced only a few days below average. Averaged annually, the 2 years differ by only 3.0°C, with 1816 having an average of 7.9°C and 2014 an average of 10.9°C.

Whilst much of Europe was exceedingly cold and wet during the summer of 1816 (in agreement with the consistent lower than average pressures, Figure 3 top), the entire North Atlantic European region (shown in Figure 3, land-only) was much closer to average (see also Figure 3). Temperatures were average in the far north of Sweden[47,48] and above normal at St Petersburg.[49] Further afield, the summer was known to be very cold in New England (3.0°C below the 1961–1990 average at Boston,[7] where it is referred to as the 'Year Without a Summer'). Recent model-constrained reconstructions indicate that over a large part of eastern North America, temperatures were 2° C below the 1700–1890 average.[50]

Estimates of the temperature impacts of Tambora over a wider spatial scale are available from marine observations.[51] The English East India Company maintained a fleet of ships trading between

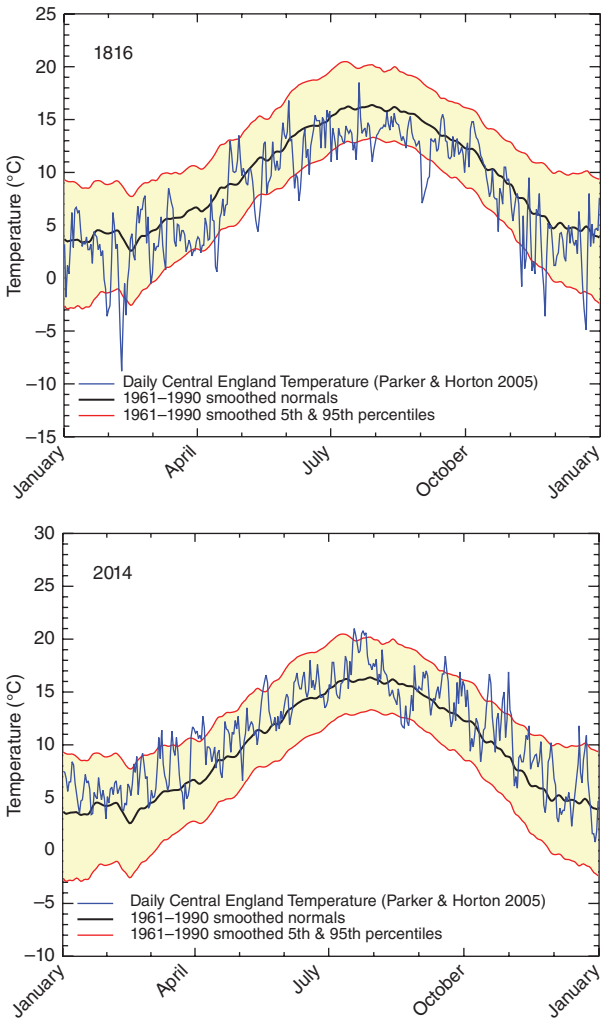

FIGURE 4 | Daily Central England temperatures for each day of the year for 1816 and 2014. Absolute temperatures are shown in blue and these can be compared with average values based on the 1961–1990 period. Apart from averages, the panels for the 2 years also show a number of percentile ranges (5/95) to illustrate how unusual some days are with respect to the distribution of individual days based on the 1961–1990 period.

Britain and southeastern Asia over a long period, and between about 1794 and 1833 many of these ships recorded noon temperatures in their logs. These observations allow annual temperature variability to be reconstructed over a large area of the Atlantic and Indian Oceans.[52] The year 1816 was the coldest year over this region, for this period, with an anomaly of about –0.6°C compared to the 1794–1833 period average (the second coldest year was 1809, also volcanically influenced by the unknown 1808/1809 eruption).

Ships' logs also provide climate information from other regions. The Hudson's Bay Company ships traveled between Britain and trading posts in Hudson's Bay in present-day Canada. These ships did not record instrumental weather observations, but their logs do provide rich information on the sea-ice conditions in Hudson Strait over the period 1751–1870. Sea-ice conditions were more severe in 1816 than in any other year in this record.[53] However, these extreme ice conditions are arguably more likely to be a result of anomalous local circulation than of large-scale temperature changes[54]—this is illustrated by the contrasting observations of William Scoresby Jr[55]: Scoresby recorded temperatures on whaling voyages in the Greenland Sea every summer from 1810 to 1818 and these observations indicate that 1816 was a relatively warm year, with less than the usual sea-ice coverage.[56] Scoresby emphasized this in a letter to Sir Joseph Banks, president of the Royal Society, stating: 'I observed on my last voyage (1817) about 2000 square leagues [18 000 square miles] of the surface of the Greenland seas, included between the parallels of 74° and 80°, perfectly void of ice, all of which disappeared within the last two years.'[57]

The instrumental observations clearly show the expected moderate large-scale cooling effect of the eruption, but also demonstrate that local effects can be quite different from the large-scale mean, and sometimes much more extreme. However, for much of the world in 1816, no instrumental observation records are currently available, so we must turn to proxy data to see what happened in those regions.

CLIMATE IMPRINT IN PROXIES AND PROXY-BASED RECONSTRUCTIONS

Apart from instrumental information, natural sources can provide further information on the summer temperature and precipitation conditions in 1816. From statistically reconstructed global or Northern Hemispheric annual mean temperature reconstructions,[2–4,58,59] it becomes obvious that 1816 was among the coldest years of the past centuries. However, the various published reconstructions disagree about the amplitude of the anomaly.[60] Compared to the 1961–1990 period, estimates range from –0.66 ± 0.24°C (standard deviation) for Northern Hemisphere temperature,[59] to –1.14°C for the temperature between 30° and 90°N[2] and –1.9°C for the Northern Hemisphere[61] (differences relative to 1785–1815 are much smaller, in the range of –0.4 to –0.8°C). It is important that in most reconstructions, the summer of 1816 followed a period with a negative temperature trend. The early 1810s were possibly already being influenced by the volcano in 1808/1809 and the lower solar insolation during the Dalton Minimum (1790–1830).

Most natural proxies (e.g., trees, lake/marine varves) and historical records[62,63] tell us about conditions in the summer, and it is this season that had the largest impact in 1816 across Europe and eastern North America. Information from tree rings provides indications about mean summer climate across the boreal forest zones of North America and Eurasia. Tree ring density is currently the most accurate proxy for the interannual temperature response to volcanic eruptions.[64] Using tree ring density data, Briffa et al.[65] showed positive temperature anomalies over parts of western America, but cold and very cold conditions around the rest of the mid latitudes of the Northern Hemisphere. This is in agreement with other tree ring-based summer temperature reconstructions that indicate strong summer cooling in 1816 in large parts of the Arctic, Northern Europe, eastern North America, and Asia.[66–68] This change in the pattern of anomalies suggests a different Rossby-wave pattern during this summer than experienced in most summers during the last 200 years.

For the winter 1816/1817, climate field reconstructions suggest a winter warming[32] similar to the temperature pattern found in composite analysis of strong volcanic eruptions during the last 500 years.[69] The reason for this warming is the North Atlantic Oscillation (NAO) which develops a positive phase after a volcanic eruption, that is, enhanced westerlies over the Atlantic European region. This dynamical response is confirmed by a recent NAO reconstruction showing a positive phase of the NAO in the winter 1816/1817.[69]

While the proxies from the Northern Hemisphere land areas generally show substantial cooling in 1816, Tambora's temperature imprint in the Southern Hemisphere appears to be substantially weaker. Hemispheric temperatures[70] do not show a significant cooling in the years following the eruption, neither do regional reconstructions from South America, Australasia, and Antarctica.[71] This weak response is generally consistent for large volcanic eruptions over the past centuries. As the Southern Hemisphere is mostly covered by oceans and its land masses are distributed more toward lower latitudes than their northern counterparts, a weaker and less immediate climatic response to volcanic eruptions is expected. Modes of internal variability, particularly of El Niño/Southern Oscillation (ENSO) and the Southern Annular Mode (SAM) have a very strong influence on the Southern Hemisphere continents. Reconstructions of the SAM[72] do not indicate a significant response to volcanic eruptions. A shift of ENSO toward an El-Niño state is found in some studies.[73] However, it does not stand out of internal variability, which is generally larger than externally forced influences.[74] This nonresponse in key circulation modes may explain the weak imprint of volcanic eruptions on continental temperatures in the Southern Hemisphere. These findings from the Southern Hemisphere are not in agreement with many climate models, which usually find volcanic cooling of similar amplitude in both hemispheres.[70] Thus, current climate models tend to overemphasize interhemispheric synchronicity by underestimating the influence of internal variability particularly in the Southern Hemisphere.[70] However, the temporal and spatial proxy data coverage is still much weaker in the Southern Hemisphere compared to Europe and North America. Hence, the apparent absence of volcanic cooling in the Southern Hemisphere may be an artifact of the low number of records able to resolve short-term peaks of climatic anomalies. Alternatively (though not supported by ice cores), the amount of aerosols reaching the Southern Hemisphere might have been smaller than assumed in these models.

Recent coral-based reconstructions of tropical SSTs in the Indian, West and East Pacific Oceans show the coldest temperatures over the past 400 years in the early 19th century.[74] While only the Indian Ocean displays a distinct interannual cold anomaly after the Tambora eruption, the decadal-scale cooling starts around 1800 in all three basins, indicating that Tambora amplifies, rather than triggers the cold period. However, the level of this amplification via volcanic eruptions cannot be quantified with reconstructions alone.

Drought reconstructions have been produced based on tree ring information from North America and for South Asia.[75,76] The *Monsoon Asia Drought Atlas* for May–September 1816 shows dry conditions in India and South Eastern Asia (weakening of the monsoon) and anomalous wet conditions in northern parts of Asia.[76] This is partly consistent with multi-proxy (tree rings, historical documentary records, and ice cores) May–September precipitation reconstructions by Feng et al.[77] The *North America Drought Atlas* for 1816 indicates wet conditions in the US Southwest (though mainly a winter response) and summer drought in the East.[75]

MODELING THE CLIMATE EFFECT OF THE TAMBORA ERUPTION

Climate models are an important tool to study the mechanisms of Tambora's impact on climate.[78–82] In fact, model results for the Tambora eruption agree with sparse observations and proxy data in some aspects.[78–81] For a more comprehensive

understanding of the mechanisms, results need to be reconciled with those found for other strong tropical volcanic eruptions. In agreement with observations and reconstructions, climate modeling studies show a drop in near-surface temperature of about 1°C over the global land areas after the Tambora eruption (Tables 1 and 2). The temperature minimum lags behind the aerosol optical depth maximum by about 2 years and gradually returns to climatological mean values after 6–10 years (Figure 5 for Northern Hemisphere temperatures). The ocean cools less than the land due to its greater heat capacity. As a result of reduced near-surface temperatures, simulated Northern hemispheric sea ice is increased and peaks 3–7 years after the eruption.[27,80,81,83]

The temperature reduction goes along with a slowdown of the global water cycle.[84,85] Global precipitation is simulated to decrease by about 0.12 mm/day after the eruption. Again, the water cycle response over land is stronger than over the ocean due to the less strong ocean cooling. Model studies of Tambora's climate effects suggest that the water cycle response mainly affected the tropical rainforest and ocean regions,[17] which is in line with model studies of other large eruptions.[26,82,86] Tambora modeling studies further imply that the change in the land-sea thermal contrast weakens the monsoonal circulations and leads to drying in monsoon regions.[87] Volcanic eruptions may also change the temperature gradient between the hemispheres. As a consequence, model simulations indicate a southward movement of the Intertropical Convergence Zone due to the increased cooling of the Northern Hemisphere landmasses as compared to the Southern Hemisphere oceans.[84,85]

TABLE 1 | Overview of Tambora modelling studies indicating the forcings used and peak temperature changes over global land areas. Estimates Indicated by ✣ Are Not Explicitly Given in the Cited Studies, But Have Been Calculated for This Publication

Study	Aerosol/Forcing	Model	Ensemble Size	Peak *DT* [K]	Duration
Tambora-only sensitivity studies:					
Stenchikov et al. (2009)[80]	3× Pinatubo optical depth (Stenchikov et al., 1998)[91]	GFDL CM2.1	10	−1.2 ± 0.1	10 years
Zanchettin et al. (2013)[94]	Crowley et al. (2008),[147] Crowley and Unterman (2013)[148]	MPI-ESM	10	−0.875 ± 0.15	8 years
Kandlbauer et al. (2013)[83]	Crowley et al. (2008)[147]	HadGEM2-ES	5	−1.0 ± 0.1	10 years
Anet et al. (2014)[89]	Arfeuille et al. (2014)[19]	SOCOL-MPIOM	3	−0.89 ± 0.35✣	6 years✣
Muthers et al. (2014)[90]	Arfeuille et al. (2014)[19]	SOCOL-MPIOM	15	−0.88 ± 0.16/ −0.80 ± 0.26✣	6–7 years✣
Tambora in transient climate simulations driven only by volcanic forcing:					
Otto-Bliesner et al. (2015)[149]	Gao et al. (2008)[22]	CESM-CAM5	5	−0.95 ± 0.12✣	6 years✣
Schurer et al. (2013)[150]	Crowley and Unterman (2013)[148]	HadCM3	3	−1.30 ± 0.05✣	7 years✣
Tambora in transient climate simulations with all major external forcings:					
This study	see Table 2	PMIP3/CMIP5 multimodel mean (see Table 2)	11	−1.05 ± 0.38	8 years

Tambora anomalies for all transient simulations were calculated relative to the less perturbed period of 1770–1799. The PMIP3/CMIP5 multimodel estimates are based on a number of transient simulations for the last millennium (CCSM4 [1], GISS-E2-R [3], IPSL-CM5A-LR [1], MPI-ESM-P [1]) and an ensemble of pre-CMIP3 simulations (COSMOS [5]). See Table 2 for the details.

TABLE 2 | Summary of the Past Millennium Simulations Used to Calculate the 'PMIP3/CMIP5 Multimodel Estimate' for Table 1

Model	Runs	Volcanic Forcing	Reference
CCSM4	1	Gao et al. (2008)[22]	Landrum et al. (2013)[151]
GISS-E2-R	3	Gao et al. (2008),[22] Crowley and Unterman (2013)[148]	Schmidt et al. (2014)[152]
IPSL-CM5A-LR	1	Ammann et al. (2007)[153]	Dufresne et al. (2013)[154]
MPI-ESM-P	1	Crowley and Unterman (2013)[148]	Jungclaus et al. (2014)[155]
COSMOS	5	Crowley et al. (2008)[141]	Jungclaus et al. (2010)[146]

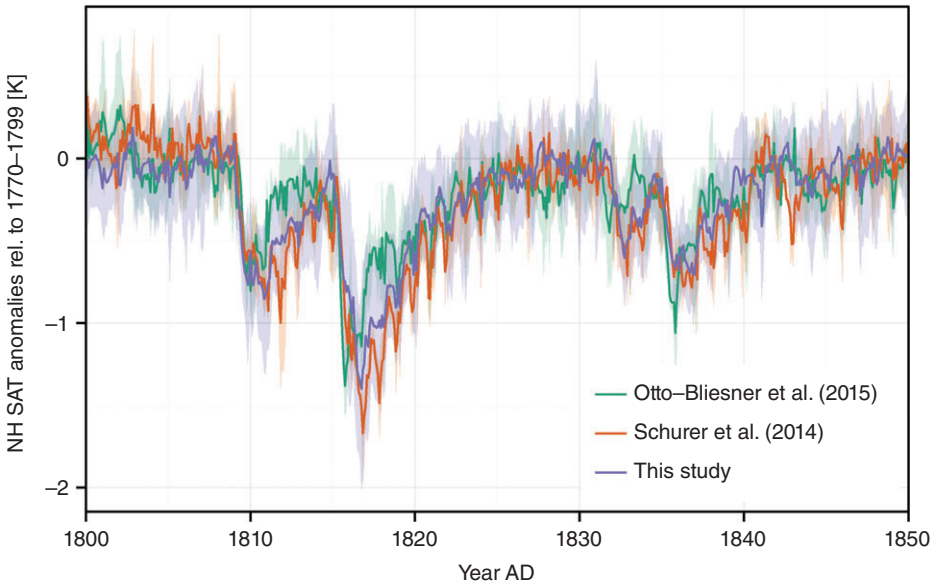

FIGURE 5 | Ensemble mean NH temperature anomalies in a number of transient simulations for the past millennium. See Table 1 for a description of the models and volcanic forcing. Anomalies were calculated relative to the period 1770–1799.

Simulated regional scale temperature and precipitation responses to large tropical eruptions at mid latitudes are heterogeneous. In summer, Western and Central Europe become cool, but not Eastern Europe.[82] Furthermore, an increase of summer precipitation is simulated over Southcentral Europe.[82,83,85] Both responses, which are also found in Tambora simulations, are consistent with observations and reconstructions.[88] The increase in precipitation might be due to a weakening and expansion of the Hadley Cell after the eruption.[82,89]

Winter precipitation is reduced in Central and Western Europe as well as over the US East Coast and large parts of the Northern Pacific after large eruptions, but increased over Northern Europe, consistent with a positive NAO.[90] This is consistent with observations.

The winter warming in Northeastern Europe and positive NAO response following strong tropical eruptions, which is well known from observations and reconstructions,[88] is no longer well reproduced by climate models.[91–93] An overall reduction of winter 500-hPa geopotential height is found in the ensemble mean of simulations, but individual model members are able to resemble the positive NAO structure of the reconstructions with increased geopotential height over Southern Europe and strongly negative anomalies over Iceland.[87,89,94] Additionally, an intensification of the polar vortex after the Tambora eruption is simulated,[90] which is hypothesized as the underlying process of the positive NAO and winter warming signal.[79,95,96]

The starting point of this mechanism is the stratosphere, where sulfate aerosols locally heat the air by absorbing terrestrial infrared as well as solar and terrestrial near-infrared radiation and reduce the transfer of short-wave radiation into lower levels. When the aerosols enter the stratosphere at tropical latitudes as for Tambora they are lifted and globally distributed by the Brewer–Dobson circulation. Initially most aerosols reside in the tropical stratosphere. This unequal distribution of aerosols leads to unequal distribution in absorbed radiation, which perturbs the meridional and vertical temperature gradients in the stratosphere. In winter, where the temperature distribution has a strong influence on the dynamics, the polar vortex is strengthened and the vertical propagation of planetary waves is altered.[95–99] The downward propagation of these pronounced dynamical changes is held responsible for the winter warming signal over Northern to Central Europe.[89,90,95–99]

In comparison to the 2.5°C warming observed in the tropical stratosphere after Mount Pinatubo,[100] a stronger warming after Tambora is likely, although the warming cannot be expected to scale linearly with the aerosol mass, because the response also depends on the microphysical properties of the aerosols.[101] Modeling studies suggest temperature anomalies about two to four times that of Pinatubo,[90,102–104] but the response depends also on the climate model and aerosol forcing applied. Similarly, an intensification of the Northern Hemisphere polar vortex can be expected[90,105] favoring positive surface temperature anomalies in parts of the

Northern Hemisphere higher latitudes in winter.[79] The strong forcing of the Tambora eruption is sufficient to induce wind anomalies that can alter the propagation of planetary waves leading to a strengthening of the polar vortex.[104]

Besides the dynamical perturbation in the stratosphere, the aerosols are also known to provide surfaces for a number of heterogeneous chemical reactions that affect the chemical composition of the stratosphere. After recent eruptions, pronounced reductions of ozone were observed,[106] which are suggested to amplify the dynamic response of the stratosphere.[107,108] For Tambora, however, the response of the ozone chemistry is assumed to be different. With low concentrations of ozone-depleting substances a slight increase of ozone concentrations is expected[109] (Figure 6) with no pronounced influences on stratospheric dynamics.[103,108] Nevertheless, the choice of the ozone dataset in climate model simulations has been shown to have substantial effect on the dynamic response to the Tambora eruption.[90]

Large volcanic eruptions like Tambora can impact the ocean. Their signals in ocean heat content may persist for decades, well beyond the lifetime of stratospheric aerosols.[74,80,110] The Tambora eruption arguably coincided with an El Niño event,[111] which was also the case for the majority of other strong tropical volcanic eruptions during the last 500 years. This has raised the question of whether volcanic eruptions can excite El Niño events.[112–114] Simulations with a climate model of intermediate complexity show that only volcanic eruptions larger than the Pinatubo size can enhance the likelihood and amplitude of an El Niño event.[73] McGregor and Timmermann[115] suggested that while the dynamical thermostat mechanism (i.e., the regulation of tropical Pacific sea surface temperatures (SSTs) through a change in the zonal temperature gradient and wind stress[116]) favors El Niño events in simplified, spatially uniform set-ups, the spatial gradients in mixed-layer depth, cloud albedo and other variables modify the response and counteract the El Niño-like response. CMIP5 historical simulations provide an opportunity to study this effect in a multimodel ensemble. While Ding et al.[117] found only a weak effect, Maher et al. found an El Niño response in the year following volcanic eruptions, and then a La Ninã 2 years later.[118]

Stenchikov et al.[80] and Ottera et al.[119] showed that major eruptions strengthen the Atlantic Meridional Overturning Circulation by a Sverdrup or more on multidecadal timescales, and consequently increase the northward heat transport. Possible mechanisms for the increase include changes in winter-time wind stress and density increases of polar surface waters. However, the models vary greatly in their simulated response.[113,120–122] Furthermore, cooling events, possibly also strong volcanic eruptions like Tambora, may trigger a coupled sea ice-ocean–atmosphere feedback in the North Atlantic and the Nordic Seas.[123]

The background state of the climate system may play an important role in the post volcanic response characteristics of the coupled sea ice-ocean–atmosphere. The decade 1810–1819 was unusually cold in the Northern Hemisphere and the tropics due to the combined effects of the unknown 1808/1809

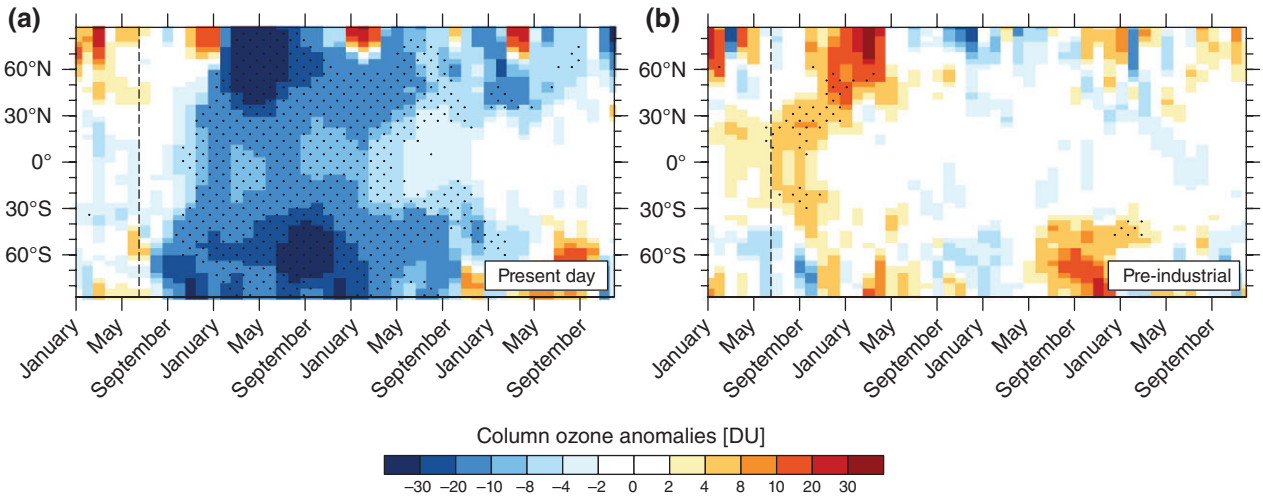

FIGURE 6 | Zonal mean column ozone changes [DU] by heterogeneous chemical reactions in an ensemble of atmosphere–ocean-chemistry climate simulations for a 4× Pinatubo eruption in a present day (left) and preindustrial (right) atmosphere (modified from Muthers et al.[103]). Vertical dashed line indicates the beginning of the eruption. Significant anomalies with respect to an ensemble of control simulations are shown by stippling.

and Tambora eruptions[124,125] and possibly decreased solar activity. Zanchettin et al.[81] demonstrated for the early 19th century that background conditions have the potential to influence the decadal climate response to strong tropical volcanic eruptions. Near-surface atmospheric and especially oceanic dynamics in a set of MPI-ESM ensemble simulations evolve significantly differently after the eruption under different background conditions (Figure 7). In particular, large interensemble member differences are found in the post-Tambora decadal evolution of oceanic heat transport and sea ice in the North Atlantic/Arctic Ocean. They reveal the existence of multiple response pathways after strong volcanic eruptions that depend on background conditions prior to the eruptions.

Zanchettin et al.[126] showed that for very large volcanic eruptions, contradictory to the Arctic, Antarctic sea ice reacts mostly to dynamical atmospheric

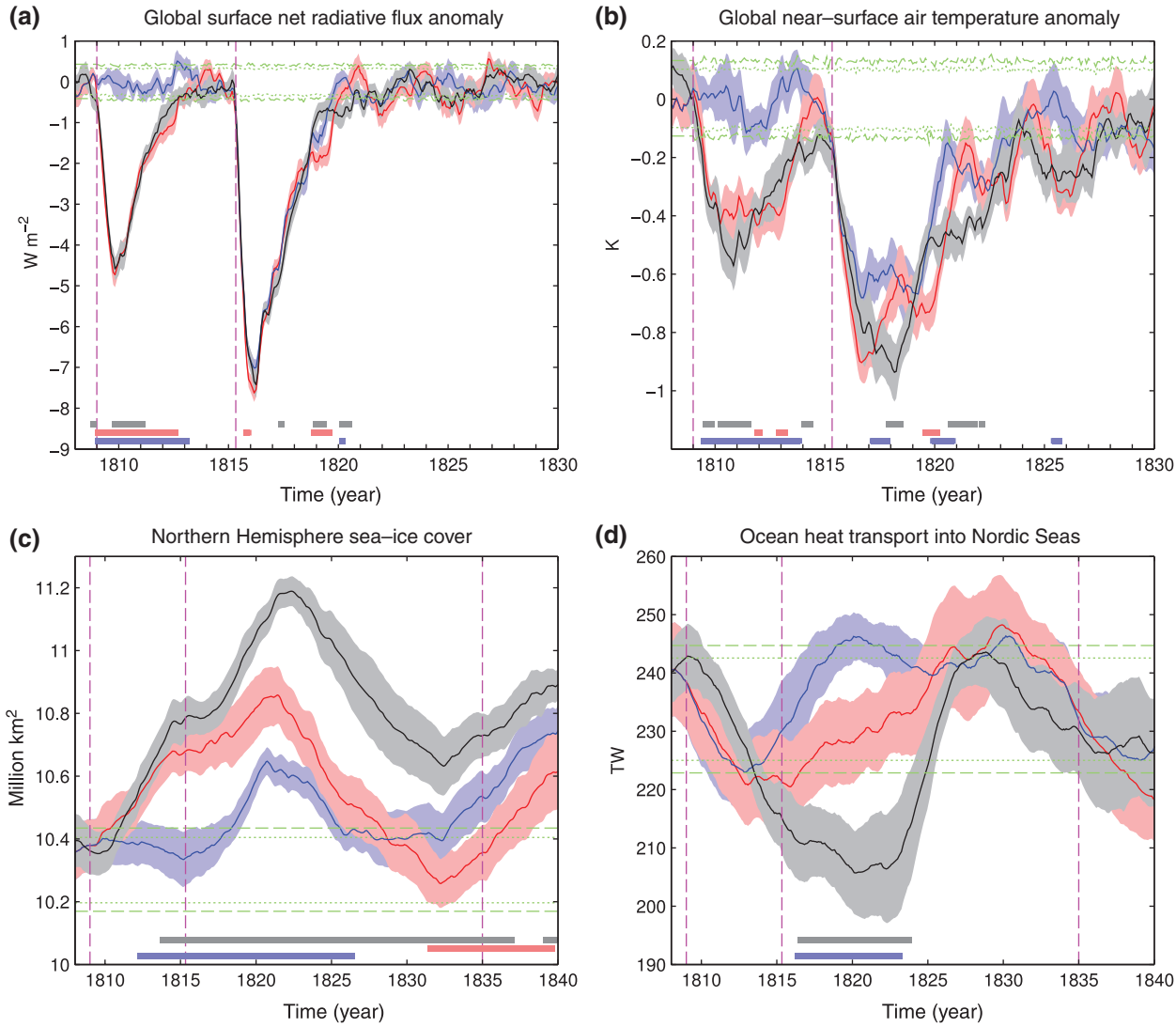

FIGURE 7 | Simulated global climate evolution of different variables in a 10 member ensemble of simulations including all natural and anthropogenic forcing (black), a 10 member ensemble with only volcanic forcing including the Tambora and the preceding 1808/1809 eruption (red), and a 10 member ensemble with only volcanic forcing without the 1808/1809 eruption (blue). The all forcing simulations are started in 1751 from initial conditions taken from the COSMOS-Mil experiments,[146] the volcanic forcing only from a control run for 800 AD conditions. Lines indicate means. Shading indicates one standard error of the mean. Green dashed lines are the 5th–95th percentile intervals for signal occurrence in the control run (see second section). The inner dotted lines are the 10th–90th percentile intervals. Magenta vertical lines indicate the occurrence of the 1808/1809 and Tambora and Cosiguina eruptions. Bottom rectangles indicate periods when there is a significant difference between an ensemble (color same as for time series) and the other two. Positive surface net radiative flux anomalies correspond to increased downward flux. The unit of the ocean heat transport is 1 TW = 10^{12} W. (Reprinted with permission from Ref 81. Copyright 2013 John Wiley and Sons)

changes initiated by the volcanically induced strengthening of the Southern Hemisphere's stratospheric polar vortex (positive SAM) and to local feedback processes. After an initial post volcanic short-lived expansion Antarctic sea ice undergoes a prolonged contraction phase. Very large volcanic forcing may therefore be a source of interhemispheric interannual-to-decadal climate variability, although the interhemispheric signature is weak in the case of historical-size eruptions like Tambora.

Large volcanic eruptions, such as Tambora, may also impact the carbon cycle.[96,127] The response of the terrestrial biosphere and ocean biogeochemistry to volcanic eruptions sensitively depends on changes in solar radiation (direct and diffuse), temperature, precipitation, fires, and atmospheric and oceanic circulation. Although the exact mechanisms causing a decrease in atmospheric CO_2 after volcanic eruptions are poorly known, it is likely that the Tambora eruption caused a decrease in atmospheric CO_2 concentration of a few ppm on decadal timescales.[83,110] It is also very likely that the volcanic emissions of CO_2 during the Tambora eruption have not significantly impacted atmospheric CO_2.[128]

In modeling and atmospheric inversion studies, focusing mainly on the Pinatubo eruption, the terrestrial biosphere has been identified as the main driver of atmospheric CO_2 changes, with minor temporary contributions of the ocean.[83,110,129–133] However, the exact mechanisms (net primary production vs respiration) by which the terrestrial biosphere drives a decadal-scale decrease in atmospheric CO_2 as well as the geographical distribution of changes are poorly known (low latitudes vs high northern latitudes). Modeling studies suggest that the sulfate aerosol-induced cooling reduces heterotrophic respiration in tropical and subtropical soils.[110,126,129–131] This increased soil carbon storage dominates over reduced litter input due to precipitation and soil moisture decrease and ultimately leads to increased terrestrial carbon uptake and decreases in atmospheric CO_2. Other studies suggest more carbon uptake in northern high latitudes,[133,134] or no change,[110] whereas some studies predict a carbon source due to decreased net primary production.[83,130,131]

The ocean initially acts as a weak carbon sink after a volcanic eruption, which is primarily due to temperature-induced increase in CO_2 solubility in low-latitude shallow waters. After the cooling signal fades, the ocean is suggested to quickly transform itself from a weak carbon sink to a weak carbon source.[110,132]

In addition to the suggested temperature and precipitation driven changes on land, several studies also suggest that an increase in diffuse radiation after volcanic eruptions may enhance the terrestrial carbon sink via enhanced net primary production.[135–137] Others argue that this effect was probably only able to compensate for the reduction in total radiation.[138] Recent laboratory experiments and direct evidence in the North Pacific also indicate that the deposition of volcanic ash on the oceanic surface may increase net primary production in the ocean,[139–141] but the impact on atmospheric CO_2 remains unclear.[142] Most current coupled climate models do not include these effects.

Although reconstructions from Antarctic ice cores do not reveal significant changes in CO_2 after the Tambora eruption, which may be due to low sampling resolution and diffusion within the archive, modeling studies suggest that atmospheric CO_2 decreased by about 6 ppm after the Tambora eruption.[83,110] The maximum decrease is delayed by a couple of years compared to changes in sulfate aerosols and atmospheric temperature. The recovery of the atmospheric CO_2 concentration takes longer than for the bulk change in temperature as longer timescales are involved in the biogeochemical cycles than in the physical processes of the atmosphere and the surface ocean. Similarly to the ocean response described above, Frölicher et al.[129] found that the carbon cycle response to volcanic eruptions critically depends on the initial conditions at the time of the eruption, with a larger atmospheric CO_2 decrease when volcanic eruptions occur during El Niño and in winter than during La Niña conditions.

CONCLUSIONS

Since 1815 the world has not been faced with an eruption of a similar strength as that of Tambora. Still, the eruption has received great attention in the sciences as it provides a rich testbed to deepen our understanding of processes during enormous eruptions and related distant impacts. Certainly mankind will be faced with such events in the future. The bicentenary of the Tambora eruption provides a perfect opportunity to reconcile our current understanding and to place the Tambora-specific findings in a broader context of processes that are relevant during and after volcanic eruptions.

During recent decades, processes during and after Tambora have been intensively investigated, narrowing down the potential volume to ~30–50 km^3.[1,17] The injection height might have been up to 40 km, but the NBH (which is relevant for the emissions) was more likely about 25 km. Still,

the volume and particularly the interhemispheric distribution of the aerosols, as well as particles sizes, are not well constrained and uncertainties about the exact values remain.

Not only does the climate forcing of the Tambora eruption have remaining uncertainties, but also the details of the climate response. Instrumental data give a detailed picture of weather and climate in specific regions following the eruption and allow addressing, for example, increased synoptic activity over Western Europe in the summer of 1816. However, the instrumental data cover only Europe and parts of North America. Nevertheless, advances in digitizing early measurements from land and oceans and an increasing network of highly resolved records from different proxy archives have led to a better global coverage of climate information in 1816 showing a widespread reduction of surface air temperatures and implications of the hydrological cycle in sensitive areas like the monsoon regions. One key finding from climate proxies is the absence of a strong Tambora signal in the extratropical Southern Hemisphere, while it is clearly expressed in the Northern Hemisphere and Tropics. This is particularly intriguing as aerosol model studies suggest that transport of aerosols was stronger toward the Southern Hemisphere than the Northern Hemisphere and ice core studies suggest equal partitioning or stronger transport toward the Southern Hemisphere.

Modeling studies allow addressing possible, physically consistent mechanisms, which may have caused the observed signal. Simulations are able to reproduce many aspects of post-Tambora climate as found in observations and proxies. The mechanisms are mostly the same as found for other strong tropical eruptions that are better constrained by observations (such as the Pinatubo eruption in 1991), but the simulated signal is stronger. However, results are sensitive to some of the uncertain parameters mentioned above. Hence, for future eruptions, one needs to take these parameters into account to cover the full uncertainty range. Moreover, climate model simulations indicate that background conditions, such as the preceding 1808/1809 eruption (unknown) and possibly the Dalton Minimum of solar activity were important for the climatic consequences of the Tambora eruption, which also needs to be taken into account when anticipating effects of future eruptions.

The effect of volcanic eruptions on the biogeochemical cycles has become an interesting research topic. In particular, the simulated carbon cycle response triggers a range of important new questions for future research.

To advance our current understanding of the dominant mechanisms behind simulated posteruption climate evolution, but also more generally, of climate dynamics and decadal variability, an international model intercomparison project on the climatic response to volcanic forcing (VolMIP)[143] has been established for the 6th cycle of the Coupled Model Intercomparison Project (CMIP6). In VolMIP, the 1815 Tambora eruption has been chosen as core experiment, to address the long-term (up to the decadal timescale) climate response to large volcanic eruptions featuring a high signal-to-noise ratio in the response of global-average surface temperature.[144] Although an improved knowledge about the climate response after the Tambora eruption is expected from the VOLMIP activity, it might still be a challenge to explain all observed regional climate anomalies.

During the past decades, our scientific understanding of the Tambora eruption has grown tremendously, and from studying the Tambora eruption, science has gained insights into many complex mechanisms operating in the climate system. Insights have also been gained on sensitivity of the system to boundary conditions, which is important for enabling society to be prepared for future eruptions. In this sense, science will undoubtedly keep learning from Tambora.

ACKNOWLEDGMENTS

This paper is dedicated to the memory of Tom Crowley, who made substantial contributions to the understanding of the role of volcanic eruptions in the Earth system. We thank NCAR and the supercomputing resources provided by NSF/CISL/Yellowstone for providing data from the CESM1 Last Millennium Ensemble Community Project. S. Muthers was supported by the Swiss National Science Foundation Sinergia Project FUPSOL2 (CRSII2-147659). R. Auchmann was supported by the Swiss National Science Foundation Project TWIST. C. Timmreck acknowledges funding from the BMBF project MIKLIP (FKZ:01LP1130A). R. Neukom is funded by the SNSF (Ambizione grant PZ00P2_154802), T. L. Frölicher acknowledges financial support from the SNSF (Ambizione grant PZ00P2_142573). P. Brohan was supported by the Joint UK DECC/Defra Met Office Hadley Centre Climate Programme (GA01101). A. Robock is supported by US National Science

Foundation grant AGS-1430051. A. Schurer and D. Zanchettin have provided model data. This paper was partly the result of a conference supported by sponsored by the Oeschger Centre for Climate Change Research of the University of Bern, the Swiss National Science Foundation, PAGES, SPARC, the Swiss Academy of Sciences, and the Johanna Dürmüller-Bol Foundation. We thank Leonie Villiger for her help in the preparation of the manuscript.

REFERENCES

1. Self S, Gertisser R, Thordarson T, Rampino MR, Wolff JA. Magma volume, volatile emissions, and stratospheric aerosols from the 1815 eruption of Tambora. *Geophys Res Lett* 2004, 31:L20608. doi:10.1029/2004GL020925.
2. Crowley TJ, Obrochta SP, Liu J. Recent global temperature 'plateau' in the context of a new proxy reconstruction. *Earth's Future* 2014, 2:281–294. doi:10.1002/2013EF000216.
3. Wilson R, D'Arrigo R, Buckley B, Buntgen U, Esper J, Frank D, Luckman B, Payette S, Vose R, Youngblut D. A matter of divergence: tracking recent warming at hemispheric scales using tree ring data. *J Geophys Res* 2007, 112:D17103.
4. D'Arrigo R, Wilson R, Tudhope A. The impact of volcanic forcing on tropical temperatures during the past four centuries. *Nat Geosci* 2009, 2: 51–56. 10.1038/ngeo393.
5. Stommel HM, Stommel E. The year without a summer. *Sci Am* 1979, 240:176–186.
6. Stothers RB. The Great Tambora eruption in 1815 and its aftermath. *Science* 1984, 224:1191–1198.
7. Harington CR. *The Year Without a Summer? World Climate in 1816*. Canadian Museum of Nature: Ottawa; 1992, 576.
8. Post JD. *The Last Great Subsistence Crisis in the Western World*. Baltimore, MD: John Hopkins; 1977, 240.
9. Luterbacher J, Pfister C. The year without a summer. *Nat Geosci* 2015, 8:246–248.
10. Krämer D. *Menschen Grasten nun mit dem Vieh. Die Letzte Grosse Hungerskrise der Schweiz 1816/17*. Basel: Schwabe; 2015, 527. ISBN: 978-3-7965-3375-4.
11. Oppenheimer C. Eruption politics. *Nat Geosci* 2015, 8:244–245.
12. Humphreys WJ. Volcanic dust and other factors in the production of climatic changes, and their possible relation to ice ages. *Bull Mount Weather Observatory* 1913, 6:1–34.
13. Dörries M. In the public eye: volcanology and climate change studies in the 20th century. *Hist Stud Phys Biol Sci* 2006, 37:87–124.
14. Bodenmann T, Brönnimann S, Hadorn GH, Kruger T, Weissert H. Perceiving, explaining, and observing climatic changes: an historical case study of the 'year without a summer' 1816. *Meteorol Z* 2011, 20:577–587. doi:10.1127/0941-2948/2011/0288.
15. Self S, Rampino MR, Newton MS, Wolff JA. Volcanological study of the great Tambora eruption of 1815. *Geology* 1984, 1984:659–663.
16. Sigurdsson H, Carey S. Plinian and co-ignimbrite tephra fall from the 1815 eruption of Tambora volcano. *Bull Volcanol* 1989, 51:243–270.
17. Kandlbauer J, Sparks RSJ. New estimates of the. Tambora eruption volume. *J Volcanol Geotherm Res* 1815, 2014:93–100.
18. Gertisser R, Self S, Thomas LE, Handley HK, van Calsteren P, Wolff JA. Processes and timescales of magma genesis and differentiation leading to the great Tambora eruption in 1815. *J Petrol* 2012, 53:271–297.
19. Arfeuille F, Weisenstein D, Mack H, Rozanov E, Peter T, Brönnimann S. Volcanic forcing for climate modeling: a new microphysics-based dataset covering years 1600–present. *Clim Past* 2014, 10:359–375. doi:10.5194/cp-10-359-2014.
20. Herzog M, Graf HF. Applying the three-dimensional model ATHAM to volcanic plumes: dynamic of large co-ignimbrite eruptions and associated injection heights for volcanic gases. *Geophys Res Lett* 2010, 37: L19807. doi:10.1029/2010GL044986.
21. Van Eaton AR, Herzog M, Wilson CJN, McGregor J. Ascent dynamics of large phreaomagmatic eruption clouds: the role of microphysics. *J Geophys Res* 2012, 117:B03203. doi:10.1029/2011JB008892.
22. Gao C, Robock A, Ammann C. Volcanic forcing of climate over the last 1500 years: an improved ice-core based index for climate models. *J Geophys Res* 2008, 113:2517–2538. doi:10.1029/2008JD010239.
23. Sigl M, McConnell JR, Layman L, Maselli O, McGwire K, Pasteris D, Dahl-Jensen D, Steffensen JP, Edwards R, Mulvaney R. A new bipolar ice core record of volcanism from WAIS divide and NEEM and implications for climate forcing of the last 2000 years. *J Geophys Res* 2013, 118:1151–1169. doi:10.1029/2012JD018603.
24. Toohey M, Krüger K, Timmreck C. Volcanic sulphate deposition to Greenland and Antarctica: a modeling sensitivity study. *J Geophys Res* 2013, 118: 4788–4800. doi:10.1002/jgrd.50428.
25. Crowley TJ. Causes of climate change over the past 1000 years. *Science* 2000, 289:270–277.

26. Timmreck C, Graf HF, Zanchettin D, Hagemann S, Kleinen T, Krüger K. Climate response to the Toba super-eruption: regional changes. *Quat Int* 2012, 258:30–44.
27. Zanchettin D, Bothe O, Timmreck C, Bader J, Beitsch A, Graf H-F, Notz D, Jungclaus JH. Inter-hemispheric asymmetry in the sea-ice response to volcanic forcing simulated by MPI-ESM (COSMOS-Mill). *Earth Syst Dyn* 2014, 5:223–242. doi:10.5194/esd-5-223-2014.
28. Kington JA. The societas meteorological palatine: an eighteenth century meteorological society. *Weather* 1974, 29:416–426.
29. Jones PD, Bradley RS. Climatic variations over the last 500 years. In: Bradley RS, Lister DH, eds. *Climate Since A.D. 1500*. London: Routledge; 1992, 649–666.
30. Luterbacher J, Dietrich D, Xoplaki E, Grosjean M, Wanner H. European seasonal and annual temperature variability, trends, and extremes since 1500. *Science* 2004, 303:1499–1503.
31. Pauling A, Luterbacher J, Casty C, Wanner H. 500 years of gridded high-resolution precipitation reconstructions over Europe and the connection to large-scale circulation. *Clim Dyn* 2006, 26:387–405.
32. Casty C, Raible CC, Stocker TF, Wanner H, Luterbacher J. European climate pattern variability since 1766. *Clim Dyn* 2007, 29:791–805.
33. Camuffo D, Jones PD, eds. *Improved Understanding of Past Climatic Variability from Early Daily European Instrumental Sources*. Dordrecht: Kluwer Academic Publishers; 2002, 392.
34. Camuffo D, Bertolin C, Barriendos M, Dominguez-Castro F, Cocheo C, Enzi S, Sghedoni M, della Valle A, Garnier E, Alcoforado MJ, et al. 500-year temperature reconstruction in the Mediterranean Basin by means of documentary data and instrumental observations. *Clim Change* 2010, 101:169–199. doi:10.1007/s10584-010-9815-8.
35. Cornes RC, Jones PD, Briffa KR, Osborn TJ. A daily series of mean sea-level pressure for London, 1692–2007. *Int J Climatol* 2012, 32:641–656. doi:10.1002/joc.2301.
36. Cornes RC, Jones PD, Briffa KR, Osborn TJ. A daily series of mean sea-level pressure for Paris, 1670–2007. *Int J Climatol* 2012, 32:1135–1150. doi:10.002/joc.2349.
37. Dominguez-Castro F, Vaquero JM, Rodrigo FS, Farrona AMM, Gallego MC, Garcıa-Herrera R, Barriendos M, Sanchez-Lorenzo A. Early Spanish meteorological records (1780–1850). *Int J Climatol* 2014, 34:593–603.
38. Kington JA. *The Weather of the 1780s over Europe*. Cambridge: Cambridge University Press; 1988, 164.
39. Briffa KR, Jones PD. The Climate of Europe during the 1810s with special reference to 1816. In: Harington CR, ed. *The Year without a Summer? World Climate in 1816*. Ottawa: Canadian Museum of Nature; 1992, 372–391.
40. Küttel M, Xoplaki E, Gallego D, Luterbacher J, Garcia-Herrera R, Allan R, Barriendos M, Jones PD, Wheeler D, Wanner H. The importance of ship log data: reconstructing North Atlantic, European and Mediterranean sea level pressure fields back to 1750. *Clim Dyn* 2010, 34:1115–1128.
41. Guevara-Murua A, Williams CA, Hendy EJ, Rust AC, Cashman KV. Observations of a stratospheric aerosol veil from a tropical volcanic eruption in December 1808: is this the Unknown 1809 eruption? *Clim Past* 2014, 10:1707–1722.
42. Auchmann R, Brönnimann S, Breda L, Bühler M, Spadin R, Stickler A. Extreme climate, not extreme weather: the summer of 1816 in Geneva, Switzerland. *Clim Past* 2012, 8:325–335. doi:10.5194/cp-8-325-2012.
43. Brugnara Y, Auchmann R, Brönnimann S, Allan RJ, Auer I, Barriendos M, Bhend J, Brázdil R, Compo GP, Cornes RC, et al. A collection of sub-daily pressure and temperature observations for the early instrumental period with a focus on the "year without a summer" 1816. *Clim Past* 2015, 11:1027–1047.
44. Pfister C. The Years without a Summer in Switzerland: 1628 and 1816. In: Harrington CR, ed. *The year without a summer? World climate in 1816*. Ottawa: Canadian Museum of Nature; 1992, 416–417.
45. Trigo RM, Vaquero JM, Alcoforado MJ, Barriendos M, Taborda J, Garcia-Herera R, Luterbacher J. Iberia in 1816, the year without a summer. *Int J Climatol* 2009, 29:99–115.
46. Parker DE, Legg TP, Folland CK. A new daily Central England Temperature Series, 1772–1991. *Int J Climatol* 1992, 12:317–342.
47. Klingbjer P, Moberg A. A composite monthly temperature record from Tornedalen in northern Sweden, 1802–2002. *Int J Climatol* 2003, 23:1465–1494.
48. Jones PD, Melvin TM, Harpham C, Grudd H, Helama S. Cool North European summers and possible links to explosive volcanic eruptions. *J Geophys Res* 2013, 118:6259–6265. doi:10.1002/jgrd.50513.
49. Jones PD, Lister DH. The daily temperature record for St. Petersburg, 1743–1996. *Clim Change* 2002, 53:253–268.
50. Brönnimann S. *Climatic Changes Since 1700*. Advances in Global Change Research Vol. 55, xv + 360 pp. Cham Heidelberg New York Dordrecht London: Springer; 2015, doi:10.1007/978-3-319-19042-6.
51. Chenoweth M. Ships' Logbooks and "The Year Without a Summer". *Bull Am Meteorol Soc* 1996, 77:2077–2094.
52. Brohan P, Rob A, Freeman E, Wheeler D, Wilkinson C, Williamson F. Constraining the

temperature history of the past millennium using early instrumental observations. *Clim Past* 2012, 8:1551–1563.

53. Catchpole AJW, Faurer MA. Summer sea ice severity in Hudson Strait, 1751–1870. *Clim Change* 1983, 5:115–139.
54. Catchpole AJW, Faurer MA. Ships' log books, sea ice, and the cold summer of 1816 in Hudson Bay and its approaches. *Arctic* 1985, 38:121–128.
55. Scoresby W. An account of the arctic regions, with a history and description of the Northern Whale-Fishery. 1820. Available at: http://books.google.co.uk/books?id=ObUUAAAAQAAJ. (Accessed May 6, 2016).
56. Brohan P, Ward C, Willetts G, Wilkinson C, Allan R, Wheeler D. Arctic marine climate of the early nineteenth century. *Clim Past* 2010, 6:315–324.
57. Barrow J. Voyages of discovery and research within the arctic regions from the year 1818 to the present time. 1846. Available at: https://books.google.ch/books?id=E_OfAAAAMAAJ&redir_esc=y. (Accessed May 6, 2016).
58. Mann ME, Zhang Z, Rutherford S, Bradley RS, Hughes MK, Shindell D, Ammann C, Faluvegi G, Ni F. Global signatures and dynamical origins of the little ice age and medieval climate anomaly. *Science* 2009, 326:1256–1260. doi:10.1126/science.1177303.
59. Frank DC, Esper J, Raible CR, Büntgen U, Trouet V, Stocker B, Joos F. Ensemble reconstruction constraints on the global carbon cycle sensitivity to climate. *Nature* 2010, 463:527–530. doi:10.1038/nature08769.
60. Masson-Delmotte V, Schulz M, Abe-Ouchi A, Beer J, Ganopolski A, González Rouco JF, Jansen E, Lambeck K, Luterbacher J, Naish T, et al. Information from paleoclimate archives. In: Stocker TF, Qin D, Plattner GK, Tignor M, Allen SK, Boschung J, Nauels A, Xia Y, Bex V, Midgley PM, eds. *Climate Change 2013: The Physical Science Basis*. Contribution of Working Group I to the Fifth Assessment Report of the IPCC. Cambridge: Cambridge University Press; 2013, 383–464.
61. Christiansen B, Ljungqvist FC. The extra-tropical northern hemisphere temperature in the last two millennia: reconstructions of low-frequency variability. *Clim Past* 2012, 8:765–786. doi:10.5194/cp-8-765-2012.
62. Dobrovolný P, Moberg A, Wilson R, Brázdil R, Pfister C, Glaser R, van Engelen A, Limanòwka D, Kiss A, Riemann D, et al. Monthly, seasonal and annual temperature reconstruction of Central Europe derived from documentary evidence since AD 1500. *Clim Change* 2010, 101:69–107.
63. Wetter O, Pfister C. Spring-summer temperatures reconstructed for northern Switzerland and southwestern Germany from winter rye harvest dates, 1454–1970. *Clim Past* 2011, 7:1307–1326.
64. D'Arrigo R, Wilson R, Anchukaitis KJ. Volcanic cooling signal in tree ring temperature records for the past millennium. *J Geophys Res* 2013, 118:9000–9010. doi:10.1002/jgrd.50692.
65. Briffa KR, Osborn TJ, Schweingruber FH, Jones PD, Shiyatov SG, Vaganov EA. Tree-ring width and density data around the Northern Hemisphere: part 2, spatio-temporal variability and associated climate patterns. *Holocene* 2002, 12:759–789.
66. Esper J, Frank DC, Timonen M, Zorita E, Wilson RJS, Luterbacher J, Holzkämper S, Fischer N, Wagner S, Nievergelt D, et al. Orbital forcing of tree-ring data. *Nat Clim Change* 2012, 2:862–866. doi:10.1038/NCLIMATE1589.
67. Tingley MP, Huybers P. Recent temperature extremes at high northern latitudes unprecedented in the past 600 years. *Nature* 2013, 496:201–205. doi:10.1038/nature11969.
68. Cook ER, Krusic PJ, Anchukaitis KJ, Buckley BM, Nakatsuka T, Sano M. Tree-ring reconstructed summer temperature anomalies for temperate East Asia since 800 CE. *Clim Dyn* 2013, 41:2957–2972. doi:10.1007/s00382-012-1611-x.
69. Ortega P, Lehner F, Swingedouw D, Masson-Delmotte V, Raible CC, Casado M, Yiou P. A multi-proxy model-tested NAO reconstruction for the last millennium. *Nature* 2015, 523:71–75.
70. Neukom R, Gergis J, Karoly DJ, Wanner H, Curran M, Elbert J, González-Rouco F, Linsley BK, Moy AD, Mundo I, et al. Inter-Hemispheric Temperature Variability over the Past Millennium. *Nat Clim Change* 2014, 4:362–367. doi:10.1038/nclimate2174.
71. Ahmed M, Anchukaitis KJ, Asrat A, Borgaonkar HP, Braida M, Buckley BM, Büntgen U, Chase BM, Christie DA, Cook ER, et al. Continental-scale temperature variability during the last two millennia. *Nat Geosci* 2013, 6:339–346.
72. Villalba R, Lara A, Masiokas MH, Urrutia R, Luckman BH, Marshall GJ, Mundo IA, Christie DA, Cook ER, Neukom R, et al. Unusual Southern Hemisphere tree growth patterns induced by changes in the Southern Annular Mode. *Nat Geosci* 2012, 5:793–798. doi:10.1038/ngeo1613.
73. Emile-Geay J, Seager R, Cane MA, Cook ER, Haug GH. Volcanoes and ENSO over the past millennium. *J Climate* 2008, 21:3134–3148.
74. Tierney JE, Abram NJ, Anchukaitis KJ, Evans MN, Giry C, Kilbourne KH, Saenger CP, Wu HC, Zinke J. Tropical sea surface temperatures for the past four centuries reconstructed from coral archives. *Paleoceanography* 2015, 30:226–252.
75. Cook ER. Long-term aridity changes in the Western United States. *Science* 2004, 306:1015–1018. doi:10.1126/science.1102586.
76. Cook ER, Anchukaitis KJ, Buckley BM, D'Arrigo RD, Jacoby GC, Wright WE. Asian monsoon failure and

megadrought during the last millennium. *Science* 2010, 328:486–489.

77. Feng S, Hu Q, Wu Q, Mann ME. A gridded reconstruction of warm season precipitation in Asia spanning the past half millennium. *J Climate* 2013, 25:2192–2204. doi:10.1175/JCLI-D-12-00099.1.
78. Vupputuri RKR. The Tambora eruption in 1815 provides a test on possible global climatic and chemical perturbations in the past. *Nat Hazards* 1992, 5:1–16. doi:10.1007/BF00127136.
79. Shindell DT, Schmidt GA, Mann ME, Falugevi G. Dynamic winter climate response to large tropical volcanic eruptions since 1600. *J Geophys Res* 2004, 109: D05104. doi:10.1029/2003JD004151.
80. Stenchikov G, Delworth TL, Ramaswamy V, Stouffer RJ, Wittenberg A, Zeng F. Volcanic signals in oceans. *J Geophys Res* 2009, 114:D16104. doi:10.1029/2008JD011673.
81. Zanchettin D, Bothe O, Graf HF, Lorenz S, Luterbacher J, Timmreck C, Jungclaus J. Background conditions influence the decadal climate response to strong volcanic eruptions. *J Geophys Res* 2013, 118:4090–4106. doi:10.1002/jgrd.50229.
82. Wegmann M, Brönnimann S, Bhend J, Franke J, Folini D, Wild M, Luterbacher J. Volcanic influence on European summer precipitation through monsoons: possible cause for "years without summer". *J Climate* 2014, 27:3683–3691. doi:10.1175/JCLI-D-13-00524.1.
83. Kandlbauer J, Hopcroft PO, Valdes PJ, Sparks RSJ. Climate and carbon cycle response to the 1815 Tambora volcanic eruption. *J Geophys Res* 2013, 118:12497–12507. doi:10.1002/2013JD019767.
84. Iles C, Hegerl GC. The global precipitation response to volcanic eruptions in the CMIP5 models. *Environ Res Lett* 2014, 9:104012.
85. Iles CE, Hegerl GC, Schurer AP, Zhang X. The effect of volcanic eruptions on global precipitation. *J Geophys Res* 2013, 118:8770–8786. doi:10.1002/jgrd.50678.
86. Joseph R, Zeng N. Seasonally modulated tropical drought induced by volcanic aerosol. *J Climate* 2011, 24:2045–2060.
87. Zhang D, Blender R, Fraedrich K. Volcanoes and ENSO in millennium simulations: global impacts and regional reconstructions in East Asia. *Theor Appl Climatol* 2013, 111:437–454.
88. Fischer EM, Luterbacher J, Zorita E, Tett SFB, Casty C, Wanner H. European climate response to tropical volcanic eruptions over the last half millennium. *Geophys Res Lett* 2007, 34:L05707. doi:10.1029/2006GL027992.
89. Anet JG, Muthers S, Rozanov EV, Raible CC, Stenke A, Shapiro AI, Brönnimann S, Arfeuille F, Brugnara Y, Beer J, et al. Impact of solar versus volcanic activity variations on tropospheric temperatures and precipitation during the Dalton Minimum. *Clim Past* 2014, 10:921–938. doi:10.5194/cp-10-921-2014.
90. Muthers S, Anet JG, Raible CC, Brönnimann S, Rozanov E, Arfeuille F, Peter T, Shapiro AI, Beer J, Steinhilber F, et al. Northern hemispheric winter warming pattern after tropical volcanic eruptions: sensitivity to the ozone climatology. *J Geophys Res* 2014, 119:1340–1355. doi:10.1002/2013JD020138.
91. Stenchikov G, Hamilton K, Stouffer R, Robock A, Ramaswamy V, Santer B, Graf HF. Arctic Oscillation response to volcanic eruptions in the IPCC AR4 climate models. *J Geophys Res* 2006, 111:D07107. doi:10.1029/2005JD006286.
92. Driscoll S, Bozzo A, Gray LJ, Robock A, Stenchikov G. Coupled Model Intercomparison Project 5 (CMIP5) simulations of climate following volcanic eruptions. *J Geophys Res* 2012, 117:D17105. doi:10.1029/ 2012JD017607.
93. Gillett NP, Fyfe JC. Annular mode changes in the CMIP5 simulations. *Geophys Res Lett* 2013, 40:1189–1193. doi:10.1002/grl.50249.
94. Zanchettin D, Timmreck C, Bothe O, Lorenz S, Hegerl G, Graf HF, Luterbacher J, Jungclaus J. Delayed winter warming: a decadal dynamical response to strong tropical volcanic eruptions. *Geophys Res Lett* 2013, 40:204–209. doi:10.1029/2012GL054403.
95. Graf HF, Kirchner I, Robock A, Schult I. Pinatubo eruption winter climate effects: model versus observations. *Clim Dyn* 1993, 9:81–93.
96. Robock A. Volcanic eruptions and climate. *Rev Geophys* 2000, 38:191–219. doi:10.1029/1998RG000054.
97. Timmreck C. Modeling the climatic effects of large explosive volcanic eruptions. *WIREs Clim Change* 2013, 3:545–564.
98. Kodera K. Influence of volcanic eruptions on the troposphere through stratospheric dynamical processes in the northern hemisphere winter. *J Geophys Res* 1994, 99:1273–1282. doi:10.1029/93JD02731.
99. Graf HF, Li Q, Giorgetta MA. Volcanic effects on climate: revisiting the mechanisms. *Atmos Chem Phys* 2007, 7:4503–4511.
100. Labitzke K, McCormick MP. Stratospheric temperature increases due to Pinatubo aerosols. *Geophys Res Lett* 1992, 19:207–210. doi:10.1029/91GL02940.
101. Timmreck C, Lorenz SJ, Crowley TJ, Kinne S, Raddatz TJ, Thomas MA, Jungclaus JH. Limited temperature response to the very large AD 1258 volcanic eruption. *Geophys Res Lett* 2009, 36:L21708. doi:10.1029/2009GL040083.
102. Arfeuille F. Impacts of large volcanic eruptions on the stratosphere and climate. PhD Thesis, *ETH Zurich*, Zurich, Switzerland, 2012.

103. Muthers S, Arfeuille F, Raible CC, Rozanov E. The impact of volcanic aerosols on stratospheric ozone and the Northern Hemisphere polar vortex: separating radiative from chemical effects under different climate conditions. *Atmos Chem Phys* 2015, 15:11461–11476. doi:10.5194/acp-15-11461-2015.

104. Bittner M, Timmreck C, Schmidt H, Toohey M, Krüger K. Sensitivity of the Northern Hemisphere winter stratosphere to the strength of volcanic eruptions. 95th American Meteorological Society Phoenix, Arizona. 2015. Available at: https://ams.confex.com/ams/95Annual/ videogateway.cgi/id/28873?recordingid=28873. (Accessed May 6, 2016).

105. Anet JG, Muthers S, Rozanov E, Raible CC, Peter T, Stenke A, Shapiro AI, Beer J, Steinhilber F, Brönnimann S, et al. Forcing of stratospheric chemistry and dynamics during the Dalton Minimum. *Atmos Chem Phys* 2013, 13:10951–10967. doi:10.5194/acp-13-10951-2013.

106. Solomon S. Stratospheric ozone depletion: a review of concepts and history. *Rev Geophys* 1999, 37:275–316. doi:10.1029/1999RG900008.

107. Stenchikov G, Robock A, Ramaswamy V, Schwarzkopf MD, Hamilton K, Ramachandran S. Arctic Oscillation response to the 1991 Mount Pinatubo eruption: effects of volcanic aerosols and ozone depletion. *J Geophys Res* 2002, 107:4803. doi:10.1029/2002JD002090.

108. Shindell DT, Schmidt GA, Miller RL, Mann ME. Volcanic and solar forcing of climate change during the preindustrial era. *J Climate* 2003, 16:4094–4107. doi:10.1175/1520-0442(2003)016<4094:VASFOC>2.0.CO;2.

109. Tie X, Brasseur G. The response of the stratospheric ozone to volcanic eruptions: sensitivity to atmospheric chlorine loading. *Geophys Res Lett* 1995, 22:3035–3038. doi:10.1029/95GL03057.

110. Frölicher TL, Joos F, Raible CC. Sensitivity of atmospheric CO_2 and climate to explosive volcanic eruptions. *Biogeosciences* 2011, 8:2317–2339.

111. McGregor S, Timmermann A, Timm O. A unified proxy for ENSO and PDO variability since 1650. *Clim Past* 2010, 5:1–17.

112. Handler P, Andsager K. Volcanic aerosols, El Niño and the Southern Oscillation. *Int J Climatol* 1990, 10:413–424.

113. Adams J, Mann ME, Ammann CM. Proxy evidence for an El Niño-like response to volcanic forcing. *Nature* 2003, 426:274–278.

114. Wilson R, Cook E, D'Arrigo R, Riedwyl N, Evans MN, Tudhope A, Allan R. Reconstructing ENSO: the influence of method, proxy data, climate forcing and teleconnections. *J Quat Sci* 2010, 25:62–78.

115. McGregor S, Timmermann A. The effect of explosive tropical volcanism on ENSO. *J Climate* 2011, 34:2178–2190.

116. Clement AC, Seager R, Cane MA, Zebiak SE. An ocean dynamical thermostat. *J Climate* 1996, 9:2190–2196.

117. Ding Y, Carton JA, Chepurin GA, Stenchikov G, Robock A, Sentman LT, Krasting JP. Ocean response to volcanic eruptions in Coupled Model Intercomparison Project 5 (CMIP5) simulations. *J Geophys Res* 2014, 119:5622–5637. doi:10.1002/2013JC009780.

118. Maher N, McGregor S, England MH, Sen Gupta A. Effects of volcanism on tropical variability. *Geophys Res Lett* 2015, 42:6024–6033. doi:10.1002/2015GL064751.

119. Otterå OH, Bentsen M, Drange H, Suo L. External forcing as a metronome for Atlantic multidecadal variability. *Nat Geosci* 2010, 3:688–694.

120. Mignot J, Khodri M, Frankignoul C, Servonnat J. Volcanic impact on the Atlantic Ocean over the last millennium. *Clim Past* 2011, 7:1439–1455.

121. Zhong Y, Miller GH, Otto-Bliesner BL, Holland MM, Bailey DA, Schneider DP, Geirsdottir A. Centennial-scale climate change from decadally-paced explosive volcanism: a coupled sea ice-ocean mechanism. *Clim Dyn* 2011, 37:2373–2387.

122. Iwi AM, Hermanson L, Haines K, Sutton RT. Mechanisms linking volcanic aerosols to the Atlantic Meridional Overturning Circulation. *J Climate* 2012, 25:3039–3051.

123. Lehner F, Born A, Raible CC, Stocker TF. Amplified inception of European Little Ice Age by sea ice-ocean–atmosphere feedbacks. *J Climate* 2013, 26:7586–7602.

124. Cole-Dai IJ, Ferris D, Lanciki A, Savarino J, Baroni M, Thiemens MH. Cold decade (AD 1810–1819) caused by Tambora (1815) and another (1809) stratospheric volcanic eruption. *Geophys Res Lett* 2009, 36:L22703. doi:10.1029/2009GL04088.

125. Schurer AP, Hegerl GC, Obrochta SP. Determining the likelihood of pauses and surges in global warming. *Geophys Res Lett* 2015, 42:5974–5982. doi:10.1002/2015GL064458.

126. Zanchettin D, Bothe O, Timmreck C, Bader J, Beitsch A, Graf HF, Notz N, Jungclaus JH. Interhemispheric asymmetry in the sea-ice response to volcanic forcing simulated by MPI-ESM (COSMOS-Mill). *Earth Syst Dyn* 2014, 5:223–242.

127. Sarmiento JL. Carbon-cycle - Atmospheric CO_2 stalled. *Nature* 1993, 365:697–698.

128. Gerlach T. Volcanic versus anthropogenic carbon dioxide. *Eos Trans AGU* 2011, 92:201. doi:10.1029/2011EO240001.

129. Frölicher TL, Joos F, Raible CC, Sarmiento JL. Atmospheric CO_2 response to volcanic eruptions: the role of ENSO, season, and variability. *Global Biogeochem Cycles* 2013, 27:239–251.

130. Jones CD, Cox PM. Modeling the volcanic signal in the atmospheric CO_2 record. *Global Biogeochem Cycles* 2001, 15:453–465.

131. Brovkin V, Lorenz SJ, Jungclaus J, Raddatz T, Timmreck C, Reick CH, Segschneider J, Six K. Sensitivity of a coupled climate-carbon cycle model to large volcanic eruptions during the last millennium. *Tellus B* 2010, 62:674–681.

132. Segschneider J, Beitsch A, Timmreck C, Brovkin V, Ilynia T, Jungclaus J, Lorenz SJ, Six KD, Zanchettin D. Impact of an extremely large magnitude volcanic eruption on the global climate and carbon cycle estimated from ensemble Earth system model simulation. *Biogeosciences* 2013, 10:669–687.

133. Bousquet P, Paylin P, Ciais P, Le Querré C, Friedlingstein P, Tans P. Regional changes in carbon dioxide fluxes of land and oceans since 1980. *Science* 2000, 290:1342–1346.

134. Lucht W, Prentice IC, Myneni RB, Sitch S, Friedlingstein P, Cramer W, Bousquet P, Buermann W, Smith B. Climate control of the high-latitude vegetation greening trend and Pinatubo effect. *Science* 2002, 296:1687–1689.

135. Farquhar GD, Roderick ML. Pinatubo, diffuse light, and the carbon cycle. *Science* 2003, 299:1997–1998.

136. Gu LH, Baldocchi DD, Wofsy SC, Munger JW, Michalsky JJ, Urbanski SP, Boden TA. Response of a deciduous forest to the Mount Pinatubo eruption: enhanced photosynthesis. *Science* 2003, 299: 2035–2038.

137. Mercado LM, Bellouin N, Stitch S, Boucher O, Huttingford C, Wild M, Cox PM. Impact of changes in diffuse radiation on the global land carbon sink. *Nature* 2009, 458:1014–1018.

138. Angert A, Biraud S, Bonfils C, Buermann W, Fung I. CO_2 seasonality indicates origins of post-Pinatube sink. *Geophys Res Lett* 2004, 31:L11103. doi:10.1029/2004GL019760.

139. Watson A. Volcanic iron, CO_2, ocean productivity and climate. *Nature* 1997, 385:587–588. doi:10.1038/385587b0.

140. Lin II, Hu C, Li YH, Ho TY, Fischer TP, Wong GTF, Wu J, Huang CW, Chu DA, Ko DS, et al. Fertilization potential of volcanic dust in the low-nutrient low-chlorophyll western North Pacific subtropical gyre: satellite evidence and laboratory study. *Global Biogeochem Cycles* 2011, 25:GB1006. doi:10.1029/2009GB003758.

141. Duggen S, Olgun N, Croot P, Hoffmann L, Dietze H, Delmelle P, Teschner C. The role of airborne volcanic ash for the surface ocean biogeochemical iron-cycle: a review. *Biogeosciences* 2010, 7:827–844.

142. Hamme RC, Webley PW, Crawford WR, Whitney FA, DeGrandpre MD, Emerson SR, Eriksen CC, Giesbrecht KE, Gower JFR, Kavanaugh MT, et al. Volcanic ash fuels anomalous plankton bloom in subarctic northeast Pacific. *Geophys Res Lett* 2010, 37:L19604. doi:10.1029/2010GL044629.

143. Zanchettin D, Timmreck C, Khodri M, Robock A, Rubino A, Schmidt A, Toohey M. A coordinated modeling assessment of the climate response to volcanic forcing, *Past Global Changes Magazine* 2015, 23:54–55 .

144. Zanchettin D, Timmreck C, Graf HF, Rubino A, Lorenz SJ, Lohmann K, Krüger K, Jungclaus JH. Bi-decadal variability excited in the coupled ocean–atmosphere system by strong tropical volcanic eruptions. *Clim Dyn* 2012, 39:419–444. doi:10.1007/s00382-011-1167-1.

145. Gertisser R, Self S. The great 1815 eruption of Tambora and future risks from large-scale volcanism. *Geology Today* 2015, 31:132–136.

146. Jungclaus JH, Lorenz SJ, Timmreck C, Reick CH, Brovkin V, Six K, Segschneider J, Giorgetta MA, Crowley TJ, Pontgratz J, et al. Climate and carbon-cycle variability over the last millennium. *Clim Past* 2010, 6:723–737.

147. Crowley TJ, Zielinski GA, Vinther B, Udisti R, Kreutz KJ, Cole-Dai J, Castellano E. Volcanism and the Little Ice Age. *Pages News* 2008, 16:22–23.

148. Crowley TJ, Unterman MB. Technical details concerning development of a 1200-yr proxy index for global volcanism. *Earth Syst Sci Data* 2013, 5:187–197.

149. Otto-Bliesner BL, Brady EC, Fasullo J, Jahn A, Landrum L, Stevenson S, Rosenbloom N, Mai A, Strand G. Climate variability and change since 850 C.E.: an ensemble approach with the Community Earth System Model (CESM). *Bull Am Meteorol Soc*. In press. doi: 10.1175/BAMS-D-14-00233.1.

150. Schurer AP, Tett SF, Hegerl GC. Small influence of solar variability on climate over the past millennium. *Nat Geosci* 2014, 7:104–108. doi:10.1038/NGEO2040.

151. Landrum L, Otto-Bliesner BL, Wahl ER, Conley A, Lawrence PJ, Rosenbloom N, Teng H. Last millennium climate and its variability in CCSM4. *J Climate* 2013, 26:1085–1111. doi:10.1175/JCLI-D-11-00326.

152. Schmidt GA, Kelley M, Nazarenko L, Ruey R, Russell GL, Aleinov I, Bauer M, Bauer SE, Bhat MK, Bleck R, et al. Configuration and assessment of the GISS ModelE2 contributions to the CMIP5 archive. *J Adv Model Earth Syst* 2014, 6:141–184. doi:10.1002/2013MS000265.

153. Ammann CM, Joos F, Schimel DS, Otto-Bliesner BL, Tomas RA. Solar influence on climate during the past

millennium: results from transient simulations with the NCAR climate system model. *Proc Natl Acad Sci* 2007, 104:3713–3718.

154. Dufresne JL, Foujols MA, Denvil S, Caubel A, Marti O, Aumont O, Balkanski Y, Bekki S, Bellenger H, et al. Climate change projections using the IPSL-CM5 Earth System Model: from CMIP3 to CMIP5. *Clim Dyn* 2013, 40:2123–2165. doi:10.1007/s00382-012-1636-1.

155. Jungclaus JH, Lohmann K, Zanchettin D. Enhanced 20th-century heat transfer to the Arctic simulated in the context of climate variations over the last millennium. *Clim Past* 2014, 10:2201–2213. doi:10.5194/cp-10-2201-2014.